

Quantized spin waves in the metallic state of magnetoresistive manganites

S. Petit¹, M. Hennion¹, F. Moussa¹, D. Lamago^{1,2}, A. Ivanov³, Y. M. Mukovskii⁴, D. Shulyatev⁴

¹ Laboratoire Léon Brillouin, CEA-CNRS, CE-SACLAY, F-91191 Gif sur Yvette Cedex, France

² Forschungszentrum Karlsruhe, INF, P. O. Box 3640, D-76021 Karlsruhe, Germany

³ Institut Laue Langevin, 156X, 38042 Grenoble cedex 9, France

⁴ Moscow State Steel and Alloys Institute, Moscow 119049, Russia

(Dated: November 7, 2018)

High resolution spin wave measurements have been carried out in ferromagnetic (F) $La_{1-x}(Sr, Ca)_xMnO_3$ with $x(Sr)=0.15, 0.175, 0.2, 0.3$ and $x(Ca)=0.3$. In all q -directions, close to the zone boundary, the spin wave spectra consist of several energy levels, with the same values in the metallic and the $x \approx 1/8$ doping ranges. Mainly the intensity varies, jumping from the lower energy levels determined in the $x \approx 1/8$ range to the higher energy ones observed in the metallic state. On the basis of a quantitative agreement found for $x(Sr) = 0.15$ in a model of ordered 2D clusters, the spin wave anomalies of the metallic state can be interpreted in terms of quantized spin waves within the same 2D F clusters, embedded in a 3D F matrix.

Charge segregation is likely the most fruitful concept to understand the extraordinary properties of manganites [1]. In spite of more than one decade of studies with recent theoretical improvements [2, 3], the doping driven transition from the orbitally ordered (OO) insulating $LaMnO_3$ to the orbital disordered (OD) metallic phase and the true nature of this metallic ferromagnetic (F) phase in cubic manganites remain very puzzling. Most of previous works have reported strong anomalies of the spin waves specially close to the zone boundary [4, 5, 6]. Their importance comes from their general character, so that they are thought to be generic features of the metallic state.

We have performed high resolution measurements of spin wave excitations in five $La_{1-x}B_xMnO_3$ samples, $B = Sr$ or Ca , for dopings covering a large part of the phase diagram (see Figure 1), from the quasimetallic (zone 2) and insulating (zone 3) parts with $x(Sr) = 0.15$ to the metallic part with $x(Sr) = 0.175, 0.2, 0.3$ and $x(Ca) = 0.3$ (zone 4). In all of them, the magnetic excitation spectrum consists of a quadratic dispersed curve in the zone center, characteristic of a three-dimensional (3D) ferromagnetic state, and wavevector-independent levels in the zone boundary. The very new result is that the energy levels observed in the metallic state have the same values whatever the doping content (zones 2, 3, 4), the temperature T or the average cation size r_a [7]. The intensity of each level depends however on x , T or r_a and is found to jump from the lower ones ($\approx 15, 22$ meV along [100]), to the upper ones ($\approx 32, 41, 51$ meV) as x increases from $\approx 1/8$ to the metallic state.

As first proposed in [8], the lower levels can be interpreted in terms of quantized spin waves within 2D F clusters of $4a$ size, considered as residual effects of the orbital ordering. For $x \approx 1/8$, a peculiar ordering of these clusters is stabilized at low T forming a ferromagnetic striped phase. The upper ones which have the main intensity in the metallic state, are assigned to their hybridization with the surrounding 3D F matrix. By defining J_{OD} and

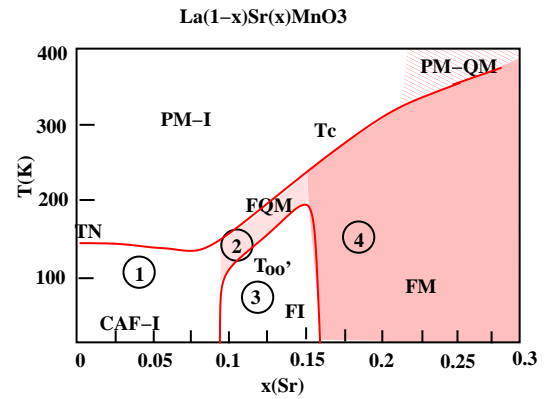


FIG. 1: (Color online) Schematic phase diagram of $La_{1-x}Sr_xMnO_3$. Zone 1: insulating canted antiferromagnetic state. Zone 2: ferromagnetic quasi-metallic state. Zone 3: insulating ferromagnetic state. Zone 4: metallic ferromagnetic state.

J_{OO} as the nearest neighbours couplings in the matrix and the clusters respectively, we find that J_{OD} increases with doping while J_{OO} does not, so that $J_{OD} \leq J_{OO}$ in zone 2 and $J_{OD} \geq J_{OO}$ in zone 4. As J_{OD} is a measure of the stiffness constant \mathcal{D} and in turn of the metallic coupling, this rapid variation with x or T is quite natural. Moreover, it explains the apparent softening of the spin wave spectrum [4, 5, 6].

Inelastic neutron scattering measurements have been carried out at the Laboratoire Léon Brillouin (1T, 2T, 4F spectrometers) and at the Institut Laue Langevin (IN8 spectrometer). To obtain a high resolution even at large energy transfer, Cu_{111} , Cu_{002} or Cu_{220} monochromators have been used. All samples have an orthorhombic structure except $La_{0.7}Sr_{0.3}MnO_3$ which is rhombohedral. For simplicity, the wavevector q is defined in pseudo-cubic indexation with **a**, **b**, **c** directions and a as lattice spacing. In the quasi-metallic and insulating states of $La_{0.85}Sr_{0.15}MnO_3$ where the magnetic coupling is anisotropic, we consider that, by continuity with

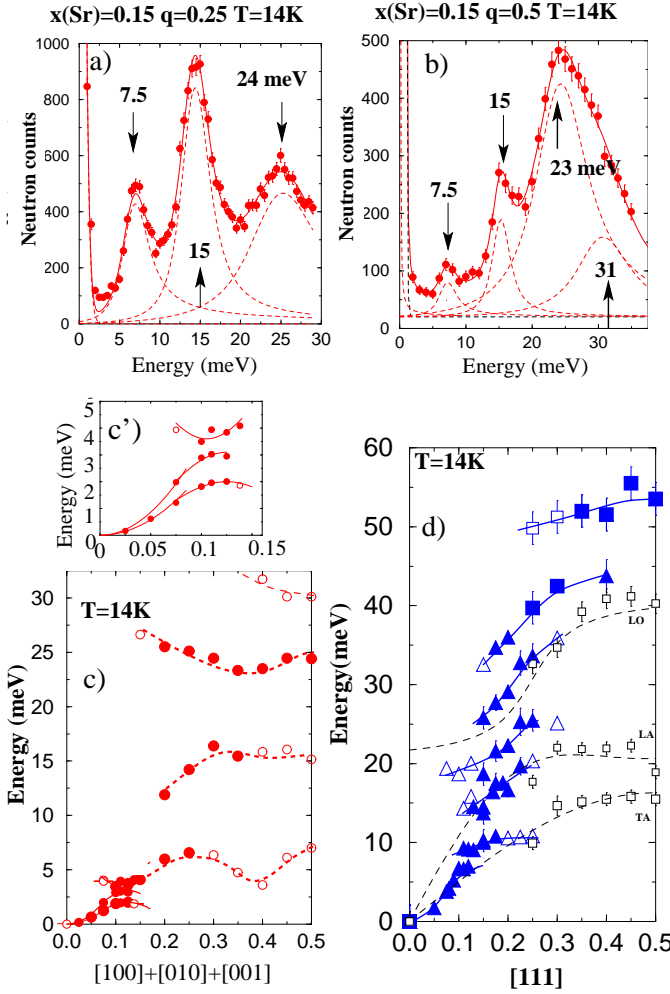


FIG. 2: (Color online) Spin waves determination in $\text{La}_{0.85}\text{Sr}_{0.15}\text{MnO}_3$ at 14K. a) and b): examples of energy spectra at $Q=(1.25,0,0)$ and $(1.5,0,0)$ resp., c) and d): spin wave spectra along $[100]+[010]+[001]$ and $[111]$ resp. with, in (c'), a zoom of the low energy part of Fig 1-c. The full (empty) color of the symbols indicates large (weak) intensity. In d), triangles (squares) indicate measurements in second (third) Brillouin zones. The black squares are phonons measured with magnons in the third Brillouin zone.

LaMnO_3 , **a** and **b** are equivalent whereas **c** is distinct. There, due to twinning, the $[100]$, $[010]$, $[001]$ directions are superposed whereas the $[111]$ direction corresponds to a single domain.

We first describe the spin dynamics in zones 2 and 3 of the phase diagram. Here, the spin wave spectrum of $x(\text{Sr}) = 0.15$ along $[1+q,0,0]$ is found to be very close to that observed for $x(\text{Sr}) = 0.125$ [8]. Below $T_C=230\text{K}$, a quadratic $E = \mathcal{D}q^2$ dispersion is observed for $q \leq 0.25$, as well as several q -independent levels for $q > 0.25$. Below $T_{OO'}=180\text{K}$, \mathcal{D} increases, whereas a gap opens at $q=0.125$. Concomitantly, the levels become q -modulated. Examples of raw data are shown at $T=14\text{K}$ in Fig 2-a and Fig 2-b. The arrows point three resolved levels at $E=7.5$,

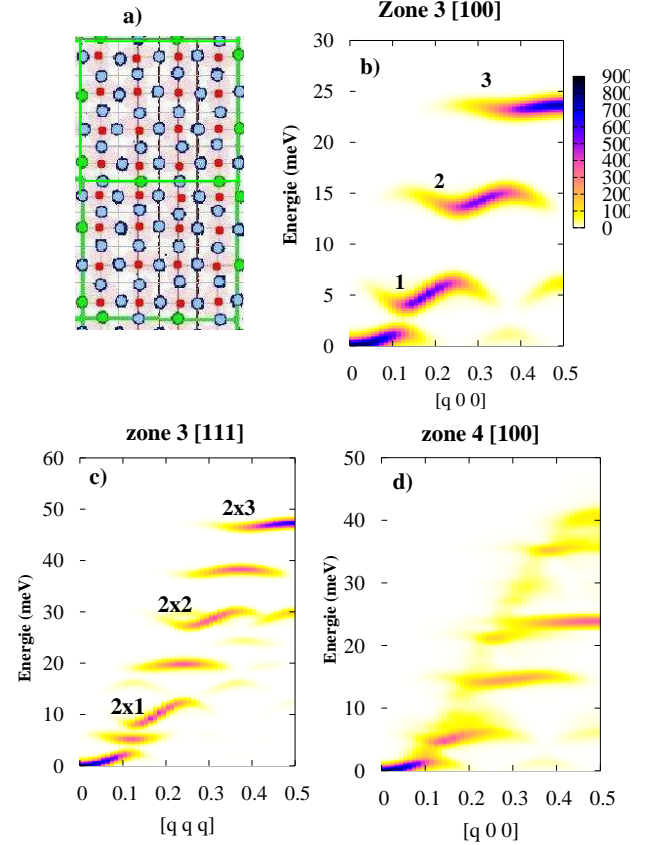


FIG. 3: (Color online) **a**): schematic drawing of two units of the 2D stripe model with red (blue and green) circles for Mn (O). **b**, **c**, **d**): calculated spin wave spectra (see the text). **b**): zone 3, along $[100]$, **c**) zone 3, along $[111]$, **d**): zone 4, along $[100]$ using 44×44 spins in **(a, b)** plane and 5 planes with cyclic boundary conditions.

15, 23 meV for $q=0.5$. The mode at $E \approx 31\text{meV}$ in the shoulder of the main peak will be discussed below. The spin wave spectrum is shown in Fig 2-c along $[100]$ and in Fig 2-d along $[111]$. The main energy values at zone boundary along $[100]$ and $[111]$ differ by a factor of ≈ 2 , which is expected for a $2D$ coupling. Actually, thanks to the high-energy resolution, the data provide evidence for two new features, not observed before [9].

i) Along $[1+q,0,0]$ with $q=0.125$, three modes are detected (cf Fig 2-c and 2-c'). The curve with a lower energy, observed only for $q < 0.15$, is assigned, from its T variation, to the **c** direction. As a result, both **a** and **b** directions are concerned with the gap opening.

ii) Along $[111]$, six levels are resolved beyond the small- q dispersion (Fig 2-d).

In a recent paper [8], we proposed a qualitative interpretation of this spin wave spectrum in terms of quantized spin waves in $2D$ $4a \times 4a$ ferromagnetic clusters. Aiming to improve this description, we propose a phe-

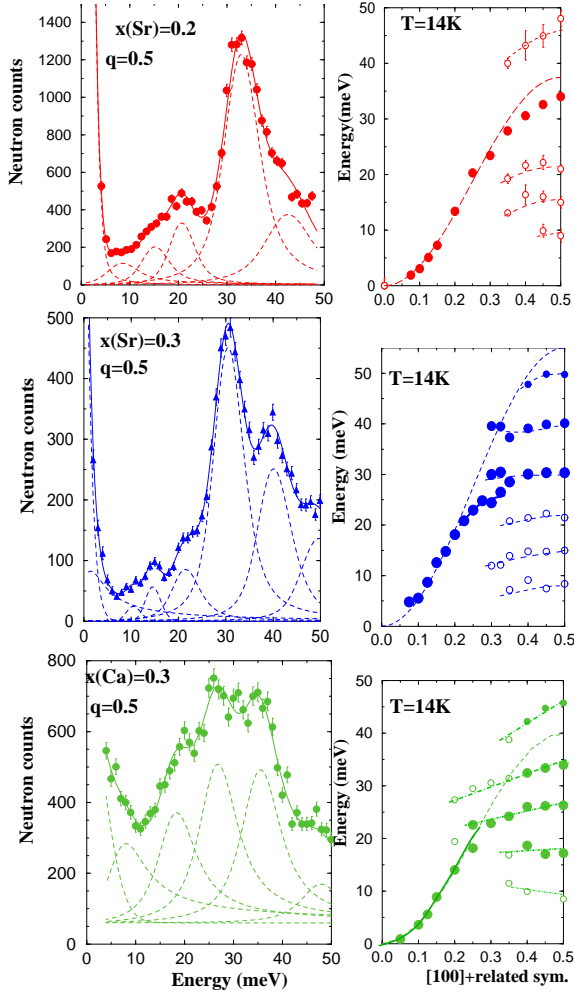


FIG. 4: (Color online) Raw data at $Q=(1.5,0,0)$ (left panel) and spin wave dispersions (right panel) determined at 14K for $La_{0.8}Sr_{0.2}MnO_3$ (top), $La_{0.7}Sr_{0.3}MnO_3$ (middle) and $La_{0.7}Ca_{0.3}MnO_3$ (bottom). The full (empty) color corresponds to large (weak) intensity. The dashed line points out the softening effect. Note the change of scale with $x(Sr)=0.15$, Fig 2.

nomenological model, assuming the existence of a long-range ordering of such clusters in (**a**, **b**) planes, resulting in the stripe picture sketched in Fig 3-a. In absence of any experimental indication, we do not consider any ordering along **c**. We then use a Heisenberg model with two next nearest neighbors (NN) coupling constants: J_{OO} and J_{inter} couple respectively Mn spins within the same clusters and across the cluster boundaries. This superstructure, also proposed in the context of high- T_C [10], implies that the holes lie, in average on the oxygen (O) atoms of the boundaries so that $x=1/8$ precisely corresponds to half-filling (see Fig 3-a). This can explain its stability on a large x range.

In this picture, the spin dynamics is that of quantized spin waves within $4a \times 4a$ clusters. 16 lev-

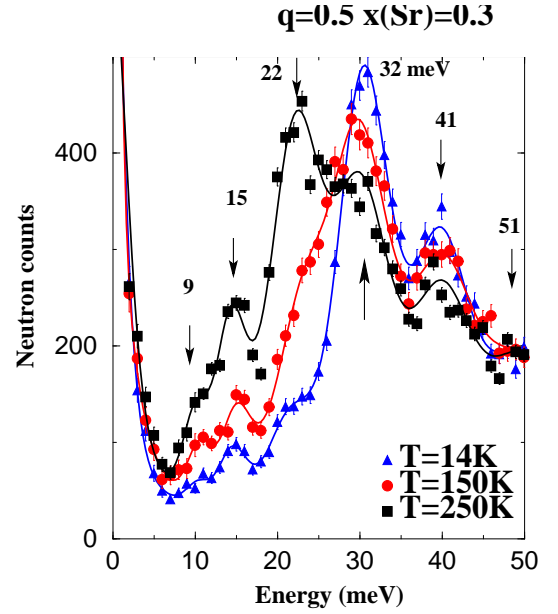


FIG. 5: (Color online) Raw data for $Q=(0,0,1.5)$ in $La_{0.7}Sr_{0.3}MnO_3$ at $T=14K$ (blue triangle), 150K (red circle) and 250K (black square).

els are expected, whose energies are given by $E_{x,y} = 4J_{OO}S \left(1 - \frac{\cos \frac{\pi x}{n} + \cos \frac{\pi y}{n}}{2}\right)$, with $n=4$ and $x,y=0, \dots, 3$. Choosing $J_{inter}=J_{OO}/5$ allows a *quantitative* description of the data, at least for $q > 0.15$ (fig 3-b, Fig 3-c). Because of the cluster square symmetry, three levels along [100] and six along [111] can be observed, in good agreement with experiment. The discrepancies which appear for $q < 0.15$ along [100] (too large gap at $q=0.125$) and along [111] (calculated energy values smaller than observed) both indicate that another F component coexists, giving rise to the nearly isotropic coupling seen for $q < 0.15$ (cf Fig 2-c'), or, equivalently, that the 2D ordering of the clusters is not very long-range [15]. Before going further, we point out that our confidence in this model arises from the agreement found for both the [100] and [111] directions. Other models have been built by considering structural observations such as the $(0,0,1/4)$ peak [11, 12]. Actually, a similar spin dynamics is observed in all the compounds which exhibit the same anomaly of resistivity (zone 3), whereas, the structural anomalies differ. An incommensurate superstructure peak is found for $x(Sr)=0.15$, whereas for $x(Ca)=0.17$ and $x(Ba)=0.15$ short-range structural defects are observed ([14] and to be published).

This new quantitative analysis of the spin wave spectrum allows to go a step further, to the true metallic state. For x at and beyond the insulator-metallic transition, the experimental observations show strong similarities with the $x \approx 1/8$ range. In fig 4, left panels show the raw data for $x(Sr)=0.2$ ($T_C=325K$) (sim-

ilar to $x(\text{Sr}) = 0.175$, $x(\text{Sr}) = 0.3$ ($T_C=370\text{K}$) and $x(\text{Ca}) = 0.3$ ($T_C=255\text{K}$) at $q=0.5$, $T=14\text{K}$. Right panels show the corresponding dispersions. Again, the spectra consist of two components : a quadratic regime near the zone center (with a weak modulated intensity around) and 2 (possibly 3) levels, namely at 15 and 22 meV, as observed in the $x \approx 1/8$ range. Additional ones are observed at higher energies, namely $E=32$ meV, ≈ 41 meV, ≈ 51 meV for $x(\text{Sr})=0.3$, and very close values for $x(\text{Ca})=0.3$ considering the slight q dependence of the levels.

Whereas the energy values of the levels are very close in all samples, their intensity shows a remarkable evolution, that we shall correlate with the evolution of the stiffness constant \mathcal{D} . A large \mathcal{D} value is associated with a strong intensity on the highest energy levels. This can be easily demonstrated by comparing $x(\text{Sr}) = 0.3$ and $x(\text{Ca}) = 0.3$ ($\mathcal{D}=200$ and 150 meV \AA^2 respectively) in Fig 4. Similarly, as \mathcal{D} decreases with increasing temperature, the intensity of the low-energy levels increases, showing again the inter-dependence of the two components. Such a variation is displayed in Fig 5 for $x(\text{Sr}) = 0.3$, where at constant energy levels, the intensity balances from upper to lower levels as T increases from 14K to 250K. The levels persist above T_C .

Along [111], new levels are observed above 50 meV up to $\approx 90 - 100$ meV, which reveal a 3D coupling. This will be reported elsewhere.

These observations in the metallic state can be understood in the framework of the model discussed above. We consider an extended version, assuming disordered 2D F clusters of $4a \times 4a$ size, embedded in a 3D F matrix. Here, an additional ferromagnetic NN coupling, J_{OD} acting between spins within the 3D medium is introduced. A qualitative agreement between the experiment and numerical simulations is obtained if $J_{OD} > J_{OO}$. Fig 3-d shows an example of calculated spin wave spectrum along [100] performed with a density of 50% of clusters, $J_{OD} = 1.75J_{OO}$ ($J_{OO}=1.7$ meV) and $J_{\text{inter}}=J_{OO}/5$. The levels reminiscent of quantized spin waves within clusters are still there. However, the hybridization with the 3D F medium results in blurring the large gaps at low q and by adding new levels at large q . Actually, the weak $E=31$ meV level detected in the $x \approx 1/8$ range below $T_{OO'}$ (Fig 2-b, 2-c and [9]) could be also due to this effect, in agreement with NMR spectroscopy [15]. Considering now the whole studied doping range, J_{OO} , which can be associated with superexchange (coupling induced by bound electrons) is found to remain approximately constant. In contrast J_{OD} , which has basically the same meaning as \mathcal{D} ($J_{OD}=\mathcal{D}/2Sa^2$) (coupling induced by hopping electrons) is found to increase with doping.

Our experiment provides a simple explanation for the so-called "softening" effect: the zone boundary energy value determined on the basis of a cosine law from the $q \approx 0$ dispersion (dashed lines in the right panels of Fig 4), clearly lies above the experimental one. This de-

scription of the data assumes however the existence of a single branch[16]. In our view, this is however not the case, as the zone boundary unravels the quantized levels. The apparent "softening" is simply due to the fact that $J_{OD} \geq J_{OO}$. Note that our interpretation reproduces the experiments in zone 2 with $J_{OD} \leq J_{OO}$.

In conclusion, instead of the previous analysis with a fourth neighbor coupling[4, 5, 6], the new data allow to describe the metallic state in terms of quantized spin waves in 2D clusters embedded in a 3D matrix. The remarkable similarities of the spin dynamics observed in several compounds, indicate that these inhomogeneities have the same origin whatever T , x or the average cation size. These new observations should be important to understand the residual resistivity [17] and the distinct magnetic time scales far from T_C [18]. Moreover, it provides a new insight around T_C where magnetic anomalies are observed [19, 20], and, hence, in the giant magnetoresistance, qualitatively similar in compounds with $x(\text{Ca})$ and $x(\text{Sr})$ ($x(\text{Sr}) < 0.4$)[21, 22], even if the "correlated polarons" play a role in Ca substituted samples [23]. In addition, this study leads to a unified picture from the CAF state with hole-rich platelets [24] to the F metallic state with hole-poor ones.

-
- [1] *Nanoscale Phase Separation and Colossal Magnetoresistance*, edited by E. Dagotto (Springer-Verlag, Berlin, 2002)
 - [2] Y. Motome and N. Furukawa Phys. Rev. B **71** 014446 (2005)
 - [3] Sanjeev Kumar et al. Phys. Rev. Lett. **97** 176403 (2006)
 - [4] Y. Endoh et al. Phys. Rev. Lett. **94**, 017206 (2005)
 - [5] F. Ye et al. Phys. Rev. Lett. **96**, 047204 (2006) and Phys. Rev. B **75** 144408 (2007)
 - [6] F. Moussa et al. Phys. Rev. B **76** 064403 (2007). Thanks to polarised neutron data (J. Fernandez-Baca, priv. comm.), the modes along [100] in $\text{La}_{0.7}\text{Ca}_{0.3}\text{MnO}_3$ can be proved to be mainly magnetic, lying on phonon energy values revising this first analysis.
 - [7] H. Y. Hwang et al. Phys. Rev. Lett. **75** 914 (1995)
 - [8] M. Hennion et al. Phys. Rev. B **73** 104453 (2006)
 - [9] F. Moussa et al. Phys. Rev. B **67** 214430 (2003)
 - [10] Boris Fine cond-mat/0404488
 - [11] Y. Yamada et al. Phys. Rev. Lett. **77** 904 (1996)
 - [12] J. Geck Phys. Rev. Lett. **95**, 236401 (2005)
 - [13] M. Hennion et al. Phys. Rev. Lett. **94** 057006 (2005)
 - [14] Pencheng Dai et al. Phys. Rev. Lett. **85** 2553 (2000)
 - [15] G. Papavassiliou et al. Phys. Rev. Lett. **96** 097201 (1996)
 - [16] N. Furukawa J. Phys. Soc. Jpn **65** 1174 (1996)
 - [17] J. M. D. Coey et al. **75** 003910 (1995)
 - [18] R. H. Heffner et al. Phys. Rev. Lett. **77**, 1869 (1996)
 - [19] J. W. Lynn et al Phys. Rev. Lett. **76** 4046 (1996)
 - [20] L. Vassiliu-Doloc et al. J. of Appl. Phys. **83** 7342 (1998)
 - [21] P. Schiffer et al. Phys. Rev. Lett. **75** 3336 (1995)
 - [22] A. Urushibara et al. Phys. Rev. **51**, 14103 (1995)
 - [23] V. Kiryukhin et al. Phys. Rev. B **70**, 214424 (2004)
 - [24] M. Hennion et al. Phys. Rev. B **61**, 9513 (2000)